

# Efficient Study of Multilayers Isosceles Triangular Microstrip Antennas

A. BEDIAF<sup>1</sup>, M. BEDRA, C. AGABA<sup>2</sup>, S. BEDRA<sup>1,3</sup>, D. BENATIA<sup>1</sup>, D. ARAR<sup>1</sup>

<sup>1</sup> L.E.A, Department of Electronics, University of Batna 2, 05000 Batna, Algeria.

<sup>2</sup> Department of Electronic, University Ferhat Abbas Setif 1, 19000 Setif, Algeria.

<sup>3</sup> Department of Industrial Engineering, University of Khenchela, 40004, Khenchela, Algeria.

E-mail : akram.bediaf@univ-batna2.dz

**Abstract** - This research paper focuses on examining an isosceles triangular micro-strip antenna placed on a multilayer substrate, either composite or suspended. The study involves determining the resonant frequency of TM modes for a patch antenna with angles of  $45^\circ-45^\circ-90^\circ$ . The resonant frequency is calculated using a precise and straightforward equation derived from an enhanced version of the cavity model. The expression is formulated in relation to stationary modes. Additionally, the paper investigates the effects of permittivity ( $\epsilon$ ) and geometrical parameters such as lateral effective width ( $S$ ) and substrate thickness ( $h$ ) on the resonant frequency

**Keywords** - microstrip antenna; isosceles; triangular patch; composite suspended.

## I. INTRODUCTION

Microstrip resonators, which were invented in the mid-20th century, are extensively utilized in contemporary electronics [1]. They find applications as filters, sensors, and antennas, primarily due to their compact size and seamless integration into printed circuits [2]. In the field of telecommunications, microstrip patch antennas are designed with various shapes, with the rectangular patch being the fundamental configuration [3]. This type of antenna consists of a conductive element in the form of a rectangle, printed on a dielectric substrate that possesses a specific relative electric permittivity  $\epsilon_r$ . This last is placed above another conductive ground plane [3] (Fig. 1).

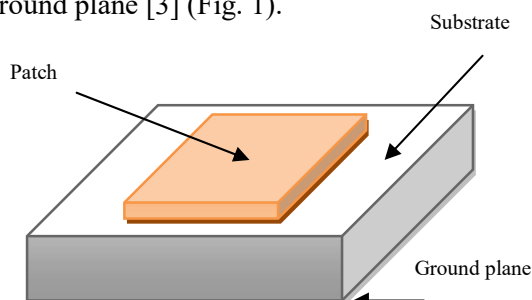


Fig. 1. Rectangular patch antenna.

Nevertheless, the primary objective of this paper is to examine the radiation efficiency of an isosceles triangular patch with angles of  $45^\circ$ ,  $45^\circ$ , and  $90^\circ$ .

This particular antenna configuration, with a  $45^\circ-45^\circ-90^\circ$  isosceles triangular shape, has received limited attention in the existing literature [4].

However, it is important to note that the previously published papers on this topic have identified certain drawbacks in their models:

- The edge effect was not properly included.
- The effect of multilayer substrates on the characteristics of a triangular patch was not considered.

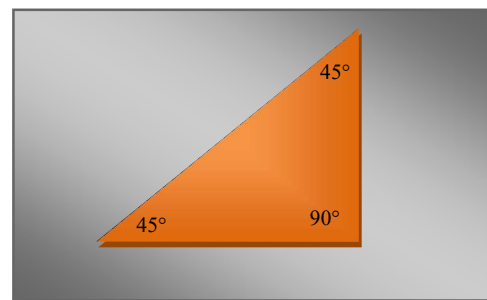


Fig. 2. Isosceles  $45^\circ-45^\circ-90^\circ$  patch antenna (front view).

Moreover, there are two approaches for analyzing printed antennas one is numeric and the other is purely analytic. Numerical approaches (Full-Wave) produce more precise findings. When compared to analytical approaches, but they necessitate the employment of strong numerical algorithms and a lengthier calculation time. They are typically based on establishing electric current distributions on the patch and ground plane here we mention four of them [5]:

- Method of moment
- The finite elements method
- The finite difference method
- The transmission line matrix method

Where else analytical approaches are based on physical electromagnetic equations, with simplified assumptions employed to generate shortened models. Though, the results are only approximations but they still very efficient when the right mathematical formulas are applied.

Among the most common analytical models for studying printed antennas we have [6]

- The transmission line model.
- The electromagnetic cavity model.

In this work the mathematical derivations are based on an improved cavity model with accurate calculation of the antenna's effective permittivity and effective dimensions. The next section describes the theory behind, having the goal of establishing a strong physical foundation for the observed occurrence. There is less documented study that shows the resonance frequency variation of a triangular microstrip antenna in case of suspended and composite substrates using the cavity technique while taking substrate permittivity (higher/lower) and antenna dimensions into account [4]. The resulting resonance frequency changes based on these characteristics have been included in this study after taking into awareness all of the aforementioned aspects.

Briefly, this paper comprises an introduction that sets the context, followed by two sections that elucidate the mathematical formulas utilized in this study and validate the underlying

assumptions. Additionally, a crucial section presents and discusses the results obtained throughout the investigation. Lastly, the paper concludes with a comprehensive summary that encompasses the entirety of the work conducted.

## II. FORMULATION THEORY

The cavity model describes the fields within the antenna as well as the radiated fields. There are no preconceived notions regarding the geometry of the radiating element, unlike the transmission line model, which is limited to rectangular patches [6]. Overall, the electric field is first considered to be restricted inside the region directly underneath the patch, separating the patch and the ground plane. This region is modelled as a rectangular hollow with an effective electric permittivity. There are six walls in the cavity: The patch and the ground plane are represented by two conducting walls (ideal electric conductors). At the patch's edge, four magnetic walls simulate an open circuit (perfect magnetic conductors). These walls operate as magnetic field conductors and interact with the electric field. This arises from the creation of charges and magnetic currents by means of reciprocity. However, if the microstrip antenna is modelled as a resonant cavity with magnetic walls, no radiation occurs since the input impedance becomes limitless [6] ( see figure.3).

To allow for an equation formulation of the stationary modes, the cavity is represented in a coordinate system  $(O,x,y,z)$  and has the following dimensions:  $L$  along the  $x$ -axis,  $W$  along the  $y$ -axis, and  $h$  along the  $z$ -axis. The assumptions made to determine the modes that exist within this cavity are as follows:

The electric walls at  $z = 0$  and  $z = h$  are ideal. The magnetic walls at  $y = 0$ ,  $y = b$ ,  $x = 0$ , and  $x = a$  are ideal.

The height  $h$  of the patch above the ground plane is much smaller than the wave length  $\lambda$  corresponding to the operating frequency of the antenna (frequency of the excited mode).

This last assumption has significant consequences. Since the tangential electric field is zero at  $z = 0$  and  $z = h$ , it can be concluded that

the field lines reaching the conductors in these two planes are orthogonal to these planes.

The thickness of the substrate ( $h = \lambda$ ) and the boundary conditions at  $z = 0$  and  $z = h$  suggest that the electric field is directed along the  $Oz$  axis and remains constant in that direction. The magnetic field has only the transverse components  $H_x$  and  $H_y$  within the region bounded by the patch and the ground plane, Therefore, we denote the internal electric field within the cavity, oriented along the  $z$ -axis, as [6].

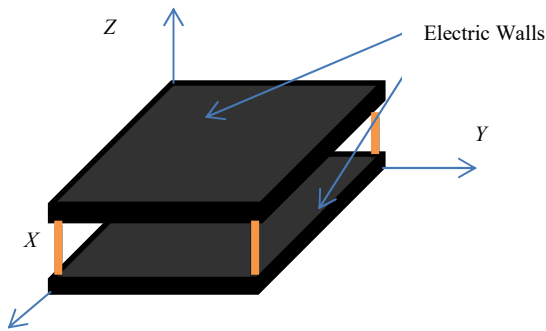


Fig. 3. Electric walls cavity model.

$$\vec{E} = E_z(x,y)\hat{k} \quad (1)$$

We utilize Maxwell's equations to derive the frequency expression of rectangular microstrip patch antenna in terms of stationary modes [6].

$$f^{mnp} = \frac{1}{2\pi\sqrt{\epsilon\mu}} \sqrt{\left(\frac{m\pi}{L}\right)^2 + \left(\frac{n\pi}{W}\right)^2 + \left(\frac{p\pi}{h}\right)^2} \quad (2)$$

At this point after conducting the general concept of cavity model we can further talk about analyzing an isosceles ( $45^\circ, 45^\circ, 90^\circ$ ) triangular patch antenna where the resonance frequency of Transfers Magnetics modes for a  $45^\circ - 45^\circ - 90^\circ$  antenna on multilayer substrates can be calculated using a simple and accurate closed-form expression [7]:

$$f_r^{mnp} = \frac{\nu_0}{2S_{eff}\sqrt{\epsilon_{reff}}} \sqrt{m^2 + n^2} \quad (3)$$

Where  $\nu_0$  is the speed of light in free space,  $\epsilon_{reff}$  is the equivalent relative permittivity of the

media beneath the patch,  $S_{eff}$  is the effective lateral length of the patch, and  $m$  and  $n$  are integers that are never be simultaneously zero, satisfying the condition  $m+n \neq 0$ .

Based on the cavity model, the resonance frequencies of a  $45^\circ - 45^\circ - 90^\circ$  triangular patch antenna with a lateral length  $S$  can be calculated using formula (4).

The triangular microstrip patch is modelled as a cavity with magnetic walls along the edges. To calculate the effective lateral length  $S_{eff}$ , most researchers [5, 7-9] have assumed that  $S_{eff}$  is independent of the modes. However, it actually depends on the mode [8, 9] due to the fact that each mode has a different edge field. The mode-dependent effective lateral length can be calculated like this.

$$S_{eff} = S + 2\sqrt{m} \frac{h}{\sqrt{\epsilon_r}} - 2\sqrt{mn} \frac{h}{\sqrt{\epsilon_r}} + 197.1 \frac{nh^2}{S\epsilon_r} \quad (4)$$

In order to provide a general formulation for multilayer structures, the multilayer structure is modeled as a single-layer structure with a substrate thickness of ( $h$ ) and an equivalent relative permittivity of the substrate  $\epsilon_{re}$ , determined under the approximations of the cavity model by:

$$\epsilon_{re} = \frac{\epsilon_{r1}\epsilon_{r2}h}{\epsilon_{r1}h_1 + \epsilon_{r2}h_2} \quad (5)$$

For a microstrip patch which is printed on a substrate with a relative permittivity of  $\epsilon_{r2}$  and thickness  $h_2$ , while maintaining a suspended or composite substrate with a relative permittivity of  $\epsilon_{r1}$  and thickness  $h_1$  above the ground plane

$$\epsilon_{reff} = \frac{\epsilon_{re} + 1}{2} + \frac{\epsilon_{re} - 1}{2} \left( \frac{1}{\sqrt{1 + 12 \frac{h}{S}}} \right) \quad (6)$$

### III. NUMERICAL RESULTS AND DISCUSSION

In this section, numerical results obtained from the cavity model for a triangular microstrip

antenna printed on suspended and composite substrates are presented.

The primary objective is to assess the precision of the method described in the previous section by comparing our results to the results offered by [4].

The comparison presented in Tables below indicates that the formulas derived from the cavity model, as discussed in the previous section, remain valid across a wide range of substrate permittivity, lateral patch width, and substrate thickness variations.

**Table 1.** Comparisons of the resonant frequencies of isosceles patch antenna on suspended substrate;

$$\epsilon_{r1} = 1; \epsilon_{r2} = 2.4; h_2 = 0.8265\text{mm}; S = 70\text{mm}.$$

$h_1$	Modes	Measured [4]	Simulated HFSS [4]	Our results
0.21	$TM_{1,0}$	1.522	1.517	1.533
	$TM_{1,1}$	2.153	2.103	2.165
	$TM_{2,0}$	3.045	3.968	3.040
	$TM_{2,1}$	3.404	3.411	3.423
0.42	$TM_{1,0}$	1.610	1.602	1.632
	$TM_{1,1}$	2.277	2.215	2.284
	$TM_{2,0}$	3.220	3.189	3.227
	$TM_{2,1}$	3.601	3.586	3.611
0.66	$TM_{1,0}$	1.663	1.648	1.701
	$TM_{1,1}$	2.352	2.297	2.347
	$TM_{2,0}$	3.326	3.226	3.355
	$TM_{2,1}$	3.719	3.713	3.711
0.8265	$TM_{1,0}$	1.694	1.690	1.734
	$TM_{1,1}$	2.396	2.334	2.363
	$TM_{2,0}$	3.389	3.278	3.413
	$TM_{2,1}$	3.789	3.796	3.736

**Table 2.** Comparisons of the resonant frequencies of isosceles patch antenna on composite substrate;

$$\epsilon_{r1} = 4.4; \epsilon_{r2} = 2.4; h_2 = 0.8265\text{mm}; S = 70\text{mm}.$$

$h_1$	Modes	Measured [4]	Simulated HFSS [4]	Our results
0.21	$TM_{1,0}$	1.296	1.297	1.294
	$TM_{1,1}$	1.833	1.806	1.833
	$TM_{2,0}$	2.592	2.549	2.569
	$TM_{2,1}$	2.899	2.911	2.898

0.42	$TM_{1,0}$	1.251	1.265	1.246
	$TM_{1,1}$	1.769	1.747	1.760
	$TM_{2,0}$	2.502	2.462	2.470
	$TM_{2,1}$	2.797	2.830	2.783
0.66	$TM_{1,0}$	1.217	1.230	1.205
	$TM_{1,1}$	1.721	1.713	1.695
	$TM_{2,0}$	2.434	2.408	2.387
	$TM_{2,1}$	2.712	2.763	2.681
0.8265	$TM_{1,0}$	1.192	1.205	1.183
	$TM_{1,1}$	1.686	1.688	1.658
	$TM_{2,0}$	2.384	3.365	2.341
	$TM_{2,1}$	2.666	2.717	2.622

To study the radiation behavior of an isosceles  $45^\circ - 45^\circ - 90^\circ$  patch antenna, we present the following results, illustrated with the graphs below.

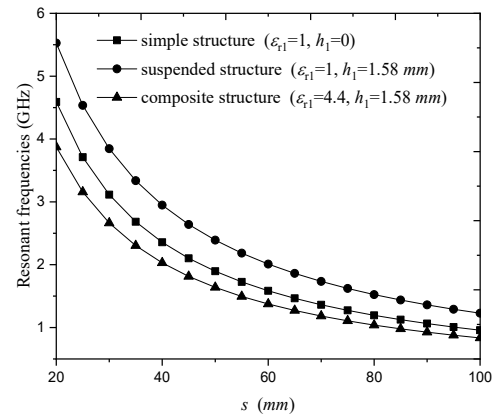


**Fig. 4.** Resonant frequency variation in function of lateral length  $S$ ;  $h_2 = 0.8265\text{mm}$ ;  $\epsilon_{r2} = 2$ .

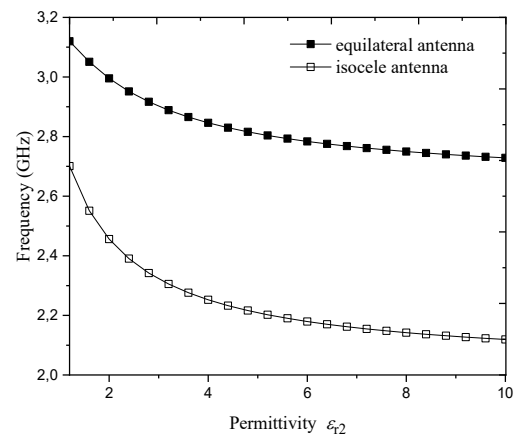


**Fig. 5.** Resonant frequency variation in function of dielectric permittivity;  $S = 50\text{mm}$ ;  $h_2 = h_1 = 0.8265\text{mm}$ .

In figure 4, we observe the variation of the resonant frequency as a function of the lateral width ( $S$ ) in different structures, with a second layer thickness ( $h_2$ ) of 0.8265 mm and an electric permittivity of 2.4.

Note that the resonant frequency starts at its maximum value within the range of 3.9 to 6 GHz for all three types of substrates. As the parameter  $S$  increases, the resonant frequency decreases proportionally until it reaches its minimum between 1 and 2 GHz when the value of  $S$  is equal to 100 mm. This clearly indicates that the lateral width ( $S$ ) of an isosceles triangular patch antenna plays a significant role in determining its characteristic resonant frequency that leads us to discuss another parameter that may also be important at this point.

In figure 5, we examine the influence of the electric permittivity of the upper substrate when it is suspended, with :

$$S = 50\text{mm}; h_1 = h_2 = 0.8265\text{mm}; \epsilon_{r1} = 1$$

From the observation of graph (figure 5), we notice that the frequency slightly decreases as the permittivity ( $\epsilon_{r2}$ ) of the Upper substrate increases.

Therefore, it is important to note that the permittivity ( $\epsilon_{r2}$ ) is another parameter that can be used to control the resonant frequency of an isosceles  $45^\circ - 45^\circ - 90^\circ$  triangular patch antenna. However, we need to understand how the permittivity acts in the case where the substrate is a composite (Figure 6).

Figure 6 shows that the influence of permittivity on the frequency follows a similar pattern as in the previous case where the substrate is suspended. However, in this case, we can observe that the influence of permittivity is even more significant.

Another parameter that is worth examining is the substrate thickness.

To examine the changes that occur in the frequency (Fig. 7) due to the substrate thickness, we analyze the graphs for varying the "h" parameter of the substrates in both composite and suspended configurations first, let's start by analyzing the effects of changing the thickness in

suspended configuration when the chosen parameters are :

$$h_2 = 0.7875, \epsilon_{r2} = 2.33, \epsilon_{r1} = 1$$

When  $h_1$  increments from 1mm to 2 mm the frequency increments quickly as well then we notice a slight decreasing in frequency when  $h_1$  parameter is above 1 mm.

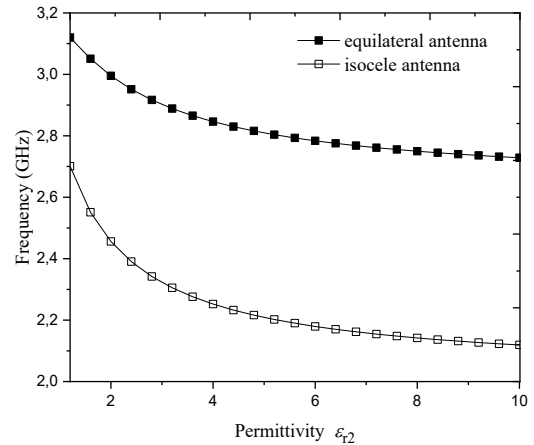


Fig. 6. Resonant frequency variation in function of dielectric permittivity;  $S = 50\text{mm}$ ;  $h_2 = 0.8265\text{mm}$ ;  $\epsilon_{r1} = \epsilon_{r2}$ .

By contrast in the case of composite substrate, though it is obvious that the change in frequency follows the same rule like previously in figure 7 but it still slower like it appears in figure 8.

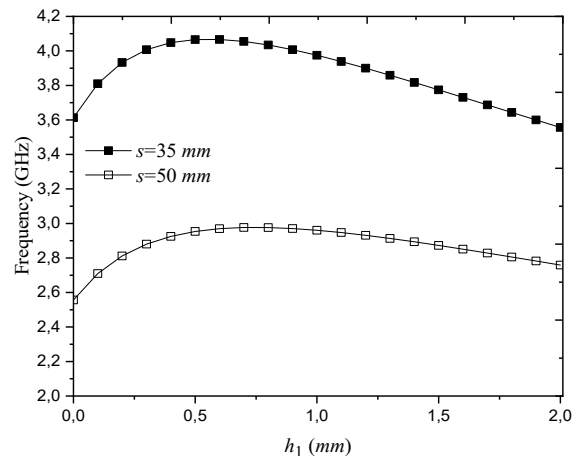
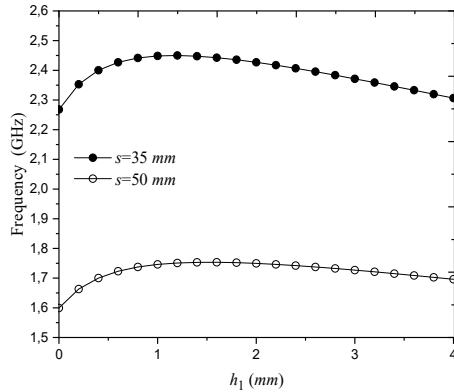


Fig. 7. Resonant frequency variation in function of thickness of substrate,  $h_2 = 0.7875\text{mm}$ ,  $\epsilon_{r1} = 1$ ,  $\epsilon_{r2} = 2.33$

As a conclusion of all the results obtained previously the resonance frequency of the antenna exhibits a significant dependency when

modifying permittivities and using thicker substrates. It is observed that thin composite substrates with higher permittivity offer favorable conditions to minimize frequency degradation.



**Fig. 8.** Resonant frequency variation in function of thickness of substrate,  $h_2 = 0.7875\text{mm}$ ,  $\epsilon_{r1} = 2.33$ ,  $\epsilon_{r2} = 3.4$

The resonance frequency is closely linked to the physical characteristics of the antenna, such as substrate thickness, lateral patch length, and dielectric constant. Furthermore, the results demonstrate that the resonance frequency increases with the enlargement of the triangular patch's thickness. These findings highlight the importance of carefully considering these factors for optimizing the performance of composite or suspended microstrip antennas

#### IV. CONCLUSION

In this paper, we have investigated the use of the cavity model for analytically modeling isosceles triangular microstrip antennas with angles of  $45^\circ - 45^\circ - 90^\circ$ . Our results demonstrate that adjusting the air gap in triangular antennas (suspended substrate) can effectively optimize the operating frequencies. It is crucial to exercise caution in the design of triangular micro-strip antennas with thin air gaps, as even a small uncertainty in the air separation adjustment can result in a significant frequency deviation. We have provided a practical solution to address this issue.

Additionally, we have determined an equivalent permittivity for the composite structure to explain the observed results. These findings are not limited to triangular patches but

can also be applied to circular and rectangular patches. In our pursuit of investigating structures that enable wireless applications, we believe that suspended and composite configurations hold great promise. Therefore, a detailed examination of the resonance phenomenon in suspended and composite configurations is of great interest.

#### V. REFERENCES

- [1] R. Colella *et al.*, "Electromagnetic characterisation of conductive 3D-Printable filaments for designing fully 3D-Printed antennas," *IET Microwaves, Antennas & Propagation*, vol. 16, no. 11, pp. 687-698, 2022.
- [2] I. Singh and V. Tripathi, "Micro strip patch antenna and its applications: a survey," *Int. J. Comp. Tech. Appl.*, vol. 2, no. 5, pp. 1595-1599, 2011.
- [3] A. K. Gupta, P. Chowdary, and M. V. Krishna, "Design of Rectangular Patch Antenna on the Hilbert Fractal-shaped High Impedance Surface," *Journal of Scientific & Industrial Research*, vol. 82, no. 02, pp. 202-209, 2023.
- [4] M. Dam and M. Biswas, "Investigation of a right-angled isosceles triangular patch antenna on composite and suspended substrates based on a CAD-oriented cavity model," *IETE Journal of Research*, vol. 63, no. 2, pp. 248-259, 2017.
- [5] C. Agaba, R. Bedra, S. Bedra, S. Benkouda, and T. Fortaki, "Study of Superconducting Equilateral Triangular Patch printed on Anisotropic Dielectric Substrates," in *2022 2nd International Conference on Advanced Electrical Engineering (ICAEE)*, 2022: IEEE, pp. 1-6.
- [6] D.-G. Fang, *Antenna theory and microstrip antennas*. CRC press, 2017.
- [7] I. Wolff and N. Knoppik, "Rectangular and circular microstrip disk capacitors and resonators," *IEEE Transactions on Microwave Theory and Techniques*, vol. 22, no. 10, pp. 857-864, 1974.
- [8] C. Gurel and E. Yazgan, "Characteristics of a circular patch microstrip antenna on uniaxially anisotropic substrate," *IEEE transactions on antennas and propagation*, vol. 52, no. 10, pp. 2532-2537, 2004.
- [9] D. Pozar, "Radiation and scattering from a microstrip patch on a uniaxial substrate," *IEEE Transactions on Antennas and Propagation*, vol. 35, no. 6, pp. 613-621, 1987.